

Synthesis of Heterobimetallic Complexes from $(\eta^4\text{-MeC}_5\text{H}_5)\text{Fe}(\text{CO})_2(\eta^1\text{-PPh}_2\text{CH}_2\text{PPh}_2)$

Ling-Kang Liu,^{*,1a,b} Lung-Shiang Luh,^{1a,b} Yuh-Sheng Wen,^{1a} Uche B. Eke,^{1a,c} and M. Adediran Mesubi^{1c}

Institute of Chemistry, Academia Sinica, Taipei, Taiwan 11529, Republic of China, Department of Chemistry, National Taiwan University, Taipei, Taiwan 10767, Republic of China, and Department of Chemistry, University of Ilorin, Ilorin, Nigeria

Received December 20, 1994[®]

The ring alkylation of $(\eta^5\text{-C}_5\text{H}_5)\text{Fe}(\text{CO})_2\text{I}$ with MeLi in the presence of $\text{PPh}_2\text{CH}_2\text{PPh}_2$ (=dppm) at -78°C yields a novel monodentate dppm complex $(\eta^4\text{-MeC}_5\text{H}_5)\text{Fe}(\text{CO})_2(\eta^1\text{-dppm})$ (**1**) that is used in this study as a mononuclear precursor for the construction of dimetallic complexes with dppm as a stabilizing backbone. Compound **1** reacts with $(\text{C}_4\text{H}_8\text{S})\text{AuCl}$ in THF at -30°C to give a heterobimetallic complex $(\eta^4\text{-MeC}_5\text{H}_5)\text{Fe}(\text{CO})_2(\mu\text{-}\eta^1\text{-}\eta^1\text{-dppm})\text{AuCl}$ (**4**), whose Au–Cl moiety could be attacked nucleophilically by MeLi to result in $(\eta^4\text{-MeC}_5\text{H}_5)\text{Fe}(\text{CO})_2(\mu\text{-}\eta^1\text{-}\eta^1\text{-dppm})\text{AuMe}$ (**5**). When complex **4** is treated with equimolar $\text{Ph}_3\text{C}^+\text{PF}_6^-$, the *endo*-H atom abstracted π complex $[(\eta^5\text{-MeC}_5\text{H}_4)\text{Fe}(\text{CO})_2(\mu\text{-}\eta^1\text{-}\eta^1\text{-dppm})\text{AuCl}]^+\text{PF}_6^-$ (**6**) is obtained. Compound **1** does not participate in the methyl migratory insertion of $(\eta^5\text{-C}_5\text{H}_5)\text{Fe}(\text{CO})_2\text{Me}$ to produce $(\eta^4\text{-MeC}_5\text{H}_5)\text{Fe}(\text{CO})_2(\mu\text{-}\eta^1\text{-}\eta^1\text{-dppm})(\eta^5\text{-C}_5\text{H}_5)\text{Fe}(\text{CO})\text{C}(\text{O})\text{Me}$ (**2**) even after refluxing in MeCN for 24 h. Interestingly, when the monodentate dppm complex **1** is allowed to react with $[\text{Rh}(\text{CO})_2\text{Cl}]_2$ in THF/*n*-hexane at room temperature, a novel heterobimetallic complex $(\eta^5\text{-MeC}_5\text{H}_4)\text{Fe}(\mu\text{-CO})_2(\mu\text{-}\eta^1\text{-}\eta^1\text{-dppm})\text{RhCl}_2$ (**9**) could be isolated in excellent yields. This immediately formed complex **9** sums up sequentially a PPh_2 ligation, an *endo*-H-atom elimination, and post rearrangements in one treatment.

Introduction

Heterobimetallic complex synthesis has been of constant interest in view of incorporation of site-selective reactivity and synergistic effects to the bimetallic system, especially the ones with catalytic potential.² Recently, a novel monodentate dppm complex— $(\eta^4\text{-MeC}_5\text{H}_5)\text{Fe}(\text{CO})_2(\eta^1\text{-PPh}_2\text{CH}_2\text{PPh}_2)$ (**1**)—has been successfully synthesized in good yields.³ The reactivity of this novel monodentate dppm toward a second metal center has been studied, aiming to construct dinuclear especially heterobimetallic systems, as reported here.

Results and Discussion

At -78°C , the reaction of equimolar $(\eta^5\text{-C}_5\text{H}_5)\text{Fe}(\text{CO})_2\text{X}$ with RLi in the presence of 1 equiv of PR'_3 has been found to cause ring alkylation, which effectively changes the $\eta^5\text{-C}_5\text{H}_5$ bonding mode in $(\eta^5\text{-C}_5\text{H}_5)\text{Fe}(\text{CO})_2\text{X}$ to $\eta^4\text{-RC}_5\text{H}_5$ bonding in $(\eta^4\text{-RC}_5\text{H}_5)\text{Fe}(\text{CO})_2(\text{PR}'_3)$.⁴ The similar ring alkylation of $(\eta^5\text{-C}_5\text{H}_5)\text{Fe}(\text{CO})_2\text{I}$ with MeLi in the presence of $\text{PPh}_2\text{CH}_2\text{PPh}_2$ (=dppm) at -78°C yields only the single-end alkylation product $(\eta^4\text{-MeC}_5\text{H}_5)\text{Fe}(\text{CO})_2(\eta^1\text{-dppm})$ (**1**) with no double-end

alkylation observed.³ There seems to be a high barrier to bring two $[(\eta^4\text{-MeC}_5\text{H}_5)\text{Fe}(\text{CO})_2]$ units into close proximity. An organometallic complex containing a pendant dppm ligand is considered to be a mononuclear precursor to react with a second metal center for the stepwise construction of a dinuclear complex in which dppm serves as a stabilizing backbone, and in many instances metal–metal interaction results.⁵ Accordingly, the novel compound **1** with pendant dppm fragment is thought to possess a potentially rich chemistry.

The phosphine-assisted Me-migratory insertion reaction of $(\eta^5\text{-C}_5\text{H}_5)\text{Fe}(\text{CO})_2\text{Me}$ has been known to be very facile.⁶ With a dangling PPh_2 in compound **1**, the **1**-induced methyl migratory insertion of $(\eta^5\text{-C}_5\text{H}_5)\text{Fe}(\text{CO})_2\text{Me}$ had been attempted, expecting the formation of a complex $(\eta^4\text{-MeC}_5\text{H}_5)\text{Fe}(\text{CO})_2(\mu\text{-}\eta^1\text{-}\eta^1\text{-dppm})(\eta^5\text{-C}_5\text{H}_5)\text{Fe}(\text{CO})\text{C}(\text{O})\text{Me}$ (**2**) in which $(\eta^4\text{-MeC}_5\text{H}_5)\text{Fe}(\text{CO})_2$ and $(\eta^5\text{-C}_5\text{H}_5)\text{Fe}(\text{CO})\text{C}(\text{O})\text{Me}$ are linked by a dppm bridge (see Scheme 1). Nonetheless, refluxing equimolar amounts of $(\eta^5\text{-C}_5\text{H}_5)\text{Fe}(\text{CO})_2\text{Me}$ and **1** in MeCN for 24 h recovered only the reactants. The IR spectroscopic data of the crude revealed four ν_{CO} bands at 2006, 1963, 1947, and 1903 cm^{-1} . Those at 2006 and 1947 cm^{-1} belonged to $(\eta^5\text{-C}_5\text{H}_5)\text{Fe}(\text{CO})_2\text{Me}$ whereas the pair at 1963 and 1903 cm^{-1} belonged to compound **1**. The ³¹P NMR spectrum had two doublets at δ 66.38 and -25.65 with $^2J_{\text{PP}} = 80.2$ Hz, comparing favorably well with those recorded for compound **1**. It was, however, remarkable to note that the novel compound **1** (mp 91–

* Author to whom correspondence should be addressed. Fax: 886-2-783 1237. E-mail: liuu@chem.sinica.edu.tw.

[®] Abstract published in *Advance ACS Abstracts*, August 15, 1995.

(1) (a) Institute of Chemistry, Academia Sinica. (b) Department of Chemistry, National Taiwan University. (c) Department of Chemistry, University of Ilorin.

(2) (a) Shore, N. E.; Hope, H. *J. Am. Chem. Soc.* **1980**, *102*, 4251.

(b) Casey, C. P.; Bullock, R. M. *Organometallics* **1982**, *1*, 1591. (c) Bahsoun, A. A.; Osborn, J. A.; Bird, P. H.; Nucciarone, D.; Peters, A. V. *J. Chem. Soc., Chem. Commun.* **1984**, 72.

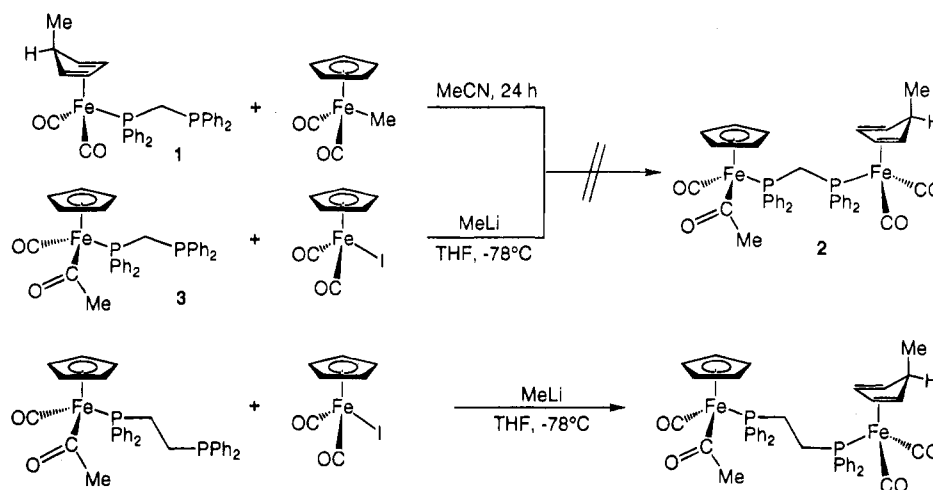
(3) Liu, L.-K.; Luh, L.-S.; Eke, U. B. *Organometallics* **1995**, *14*, 440.

(4) (a) Liu, L.-K.; Luh, L.-S. *Organometallics* **1994**, *13*, 2816. (b) Luh, L.-S.; Liu, L.-K. *Bull. Inst. Chem., Acad. Sinica* **1994**, *41*, 39.

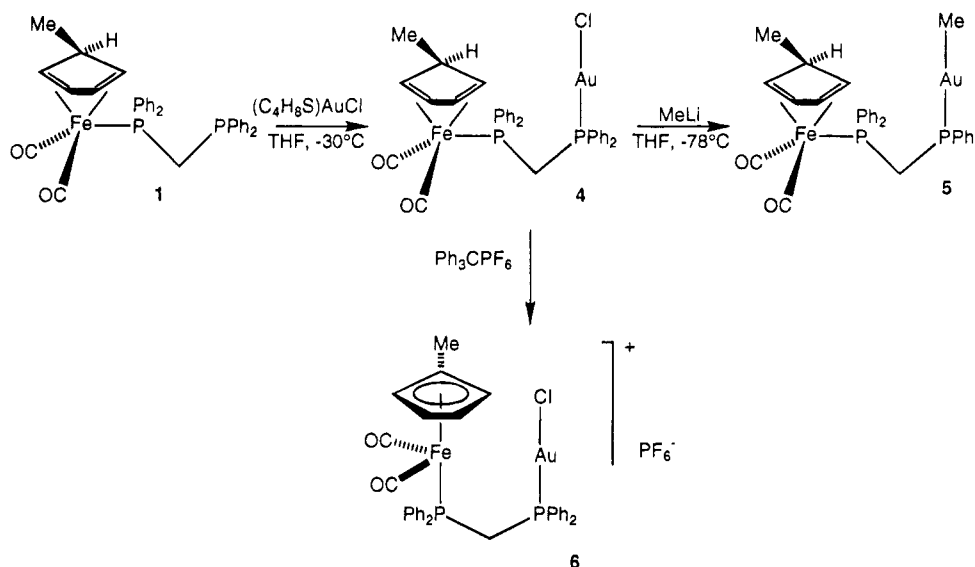
(5) (a) Puddephatt, R. J. *Chem. Soc. Rev.* **1983**, *12*, 99. (b) Chaudret, B.; Delavaux, B.; Poilblanc, R. *Coord. Chem. Rev.* **1988**, *86*, 191. (c) Braunstein, P.; de Meric de Bellefon, C.; Oswald, B. *Inorg. Chem.* **1993**, *32*, 1638. (d) Braunstein, P.; Knorr, M.; Strampfer, M.; Dusausoy, Y.; Bayeul, D.; DeCian, A.; Fischer, J.; Zanello, P. *J. Chem. Soc., Dalton Trans.* **1994**, 1533.

(6) Bibler, J. P.; Wojcik, A. *Inorg. Chem.* **1966**, *5*, 889.

Scheme 1



Scheme 2



92 °C) and $(\eta^5\text{-C}_5\text{H}_5)\text{Fe}(\text{CO})_2\text{Me}$ (mp 80–83 °C) withstood the refluxing temperature of MeCN (bp 81 °C) for 24 h. In a separate experiment, the ring alkylation reaction³ of $(\eta^5\text{-C}_5\text{H}_5)\text{Fe}(\text{CO})_2\text{I}$ with MeLi in the presence of $(\eta^5\text{-C}_5\text{H}_5)\text{Fe}(\text{CO})\text{C}(\text{O})\text{Me}(\eta^1\text{-dppm})$ (**3**) (as a phosphine source) at –78 °C was also performed in a hope to produce **2** (see Scheme 1). Synthetic manipulations and chromatography following the usual low-temperature, three-component reaction procedure gave just small amounts of orange, waxy, de-insertion complex $(\eta^5\text{-C}_5\text{H}_5)\text{Fe}(\text{CO})_2\text{Me}$ along with three other low-yield compounds with spectroscopic data (IR, ³¹P, and ¹H NMR) not informative enough for identification.⁷ Similar strategy works for the dppe analog with excellent yields (see also Scheme 1), however.⁸

In addition to the attempts to construct above mentioned dppm-linked diiron complexes, other dinuclear systems were explored. For instance, equimolar amounts of **1** and $(\text{C}_4\text{H}_8\text{S})\text{AuCl}$ [or $(\text{Me}_2\text{S})\text{AuCl}$] were reacted in THF at –30 °C to give the heterobimetallic complex $(\eta^4\text{-MeC}_5\text{H}_5)\text{Fe}(\text{CO})_2(\mu\text{-}\eta^1:\eta^1\text{-dppm})\text{AuCl}$ (**4**) in 68.7% yields

(Scheme 2). After purification on a column of nonactivated alumina, crystals suitable for X-ray diffraction were grown from a $\text{CH}_2\text{Cl}_2/n\text{-hexane}$ mixture. A $\text{d}^{10}\text{-Au}_2$ fragment has formed successfully at the originally pendant PPh_2 end. The ³¹P NMR resonance of $\text{P}(\text{Au})$ at δ 19.06 shows a δ 44.66 downfield coordination shift (cf. δ –25.60 in compound **1**). The 14 electron $\text{P}(\text{Au})$ unit is known a common configuration of $\text{d}^{10}\text{-Au}$ core.⁹ The ³¹P NMR chemical shifts have been reported ranging δ 14.6–32.3 in $\text{P}(\text{Au})$ systems where a bridging dppm is present.¹⁰ In complex **4**, the ³¹P NMR chemical shift of PPh_2 connected to Fe is virtually unchanged at δ 65.78 (cf. δ 66.38 in compound **1**). The IR spectrum of **4** reveals the presence of two terminal CO stretching bands at 1966 and 1906 cm^{-1} (1963 and 1902 cm^{-1} in the parent compound), exhibiting a slight reduction in electron density at the Fe center. The ¹H NMR spectrum is made up of multiplets at δ 7.5–7.3

(7) The species found are more than likely the decomposed/degraded products, for instance, dppm, $[(\eta^5\text{-C}_5\text{H}_5)\text{Fe}(\text{CO})_2]_2$, etc., in addition to $(\eta^5\text{-C}_5\text{H}_5)\text{Fe}(\text{CO})_2\text{Me}$.

(8) Luh, L.-S.; Liu, L.-K. *Organometallics* **1995**, *14*, 1514.

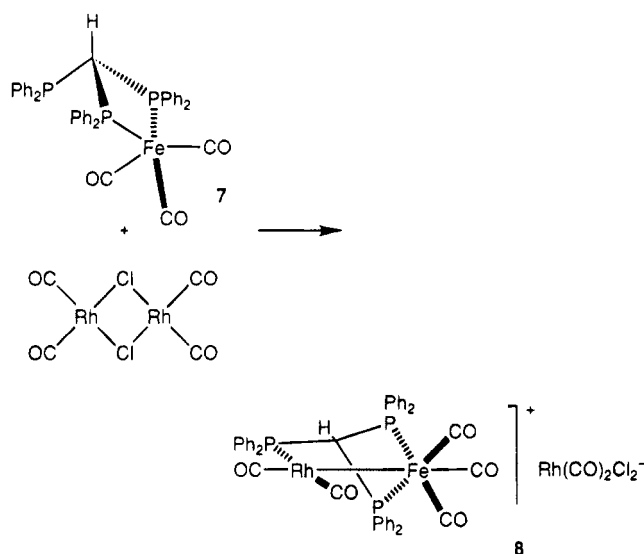
(9) (a) Hitchcock, P. B.; Pye, P. L. *J. Chem. Soc., Dalton Trans.* **1977**, 1457. (b) Cooper, M. K.; Mitchell, L. E.; Hendrick, K.; McPartlin, M.; Scott, A. *Inorg. Chim. Acta* **1984**, *84*, L9. (c) Hill, D. T.; Girard, G. R.; McCabe, F. L.; Johnson, R. K.; Stupik, P. D.; Zhang, J. H.; Reiff, W. M.; Egleston, D. S. *Inorg. Chem.* **1989**, *28*, 3529. (d) Ni Dhubhghaill, O. M.; Sadler, P. J.; Kuroda, R. *J. Chem. Soc., Dalton Trans.* **1990**, 2913. (e) Schmidbauer, H.; Stutzer, A.; Bissinger, P. *Z. Naturforsch.* **1992**, *47B*, 640. (f) Schmidbauer, H.; Bissinger, P.; Lachmann, J.; Steigelmann, O. *Z. Naturforsch.* **1992**, *47B*, 1711.

for Ph protons; δ 4.80, 2.56, and 2.27 for the H_{2,3}, H₅, and H_{1,4} atoms in ratio of 2:1:2; δ 3.39 for methylene H atoms; and a doublet at δ 0.27 for Me protons. The ¹³C NMR data is in accordance with the pattern and assignments observed for the precursor compound **1**. The observed spectroscopic data are in agreement with the X-ray-deduced structure.

The Au–Cl moiety of complex **4** is easily subjected to a nucleophilic substitution. When treated with MeLi at -78°C in THF for 4 h, complex **4** proceeds smoothly, as shown in Scheme 2, with a replacement of Cl by Me to give $(\eta^4\text{-MeC}_5\text{H}_5)\text{Fe}(\text{CO})_2(\mu\text{-}\eta^1\text{:}\eta^1\text{-dppm})\text{AuMe}$ (**5**) in 74.0% yields. By comparison of the IR and ³¹P NMR data of **4** and **5**, it is concluded that no significant chemistry takes place around the Fe coordination sphere when MeLi reacts with **4**. For instance, the ν_{CO} bands at 1966 and 1906 cm^{-1} in the precursor are found at 1962 and 1902 cm^{-1} in the product. The ³¹P NMR studies of **5** reveal the P–(Fe) resonance at δ 65.36 and that of P–(Au) is at δ 34.30 whereas in **4** P–(Fe) resonances at δ 65.78 and P–(Au) at δ 19.04. The 15.26 δ units downfield shift of ³¹P–(Au) resonance on formation of **5** is regarded as a direct evidence for the Me[–] nucleophilic substitution at the Au atom. The ¹H and ¹³C NMR data of **5** are very similar to those of **4**, the only difference being the presence of the newly added Me on Au atom—at δ 0.02 ($^3J_{\text{PH}} = 8.1$ Hz) in ¹H NMR and at δ 1.02 in ¹³C NMR. The observed spectroscopic data also conform to the X-ray structure in the solid state.

The *endo* H-atom of the $\eta^4\text{-MeC}_5\text{H}_5$ ring has been confirmed to be hydridic in nature. When complex **4** was treated with equimolar $\text{Ph}_3\text{C}^+\text{PF}_6^-$ in CH_2Cl_2 at 0°C , a novel complex $[(\eta^5\text{-MeC}_5\text{H}_4)\text{Fe}(\text{CO})_2(\mu,\eta^1\text{:}\eta^1\text{-dppm})\text{-AuCl}]^+\text{PF}_6^-$ (**6**) resulted in 86% yields (Scheme 2). A hydridic H-atom is known to be abstracted by a triphenylmethane cation Ph_3C^+ to produce a triphenylmethane Ph_3CH .¹¹ The bonding mode of the $(\eta^4\text{-MeC}_5\text{H}_5)$ ring in **4** thus changes to $(\eta^5\text{-MeC}_5\text{H}_4)$ in **6**. Such a transformation is equivalent to the oxidation of the d⁸-Fe in zero valence to a d⁶-Fe in +2 valence, the neutral complex **4** finalizing as the cationic complex **6**. A reduction of electron density at the Fe center in **6** is evidenced with a blue shift of the IR ν_{CO} bands from 1966 and 1906 cm^{-1} in **4** to 2050 and 2007 cm^{-1} in **6**. Complex **6** reveals in ³¹P NMR the presence of three nonequivalent P atoms in the molecule: P–(Fe), δ 56.48; P–(Au), δ 20.68; and P–(F), δ –143.38 (septet, $^1J_{\text{PF}} = 711$ Hz). The assignment of the P–(Fe) and P–(Au)

Scheme 3



peaks has been done by comparison with those of the precursor **4**. In the ¹H NMR spectrum, the features of $(\eta^4\text{-MeC}_5\text{H}_5)$ ring in **4** are now replaced by two peaks at δ 4.9 (2H) and 4.8 (2H) of the new $(\eta^5\text{-MeC}_5\text{H}_4)$ ring in **6**. The assignment of these peaks to H_{2,5} and H_{3,4} atoms, however, are still not unambiguous. The methylene H atoms of dppm and the methyl H atoms of the $\eta^5\text{-MeC}_5\text{H}_4$ ring in **6** occur at δ 4.01 and 1.83, respectively, both resonances experiencing substantial downfield shifts from δ 3.37 and 0.27 in **4**. The ¹³C NMR data are also consistent with the assigned formula of complex **6**.

With $\text{Ph}_3\text{C}^+\text{PF}_6^-$ externally eliminating the *endo*-H atom of **4**, the resulting **6** shows no Fe–Au bond formation because neither $^{2+3}J_{\text{PP}}$ coupling nor ³¹P shift due to a ring formation could be recorded— δ 19.04 (s) vs δ 20.68 (s) before and after *endo*-H atom abstraction experiment. The P–(Au) local environment remains unchanged in the conversion from **4** to **6**. The experimental results suggest that, in the Fe–Au heterobimetallic system, the monodentate dppm ligation to the Au center followed by *endo*-H atom elimination of the $(\eta^4\text{-MeC}_5\text{H}_5)$ ring does not lead to an Fe–Au bond formation.

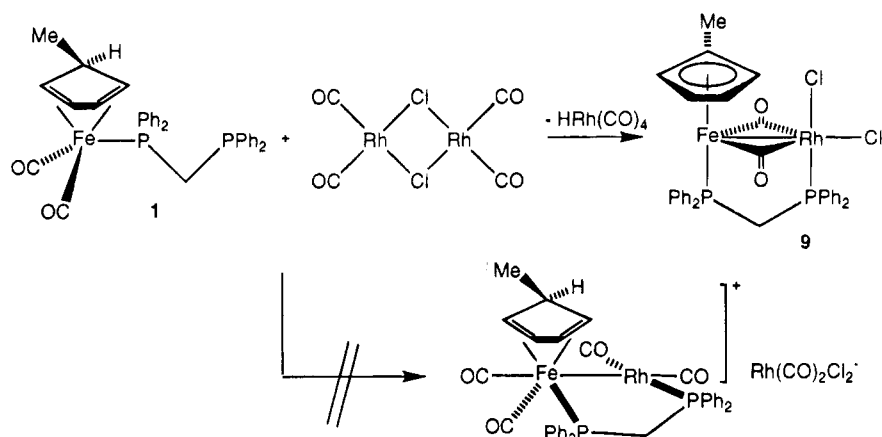
In the literature, Osborn *et al.* reacted $[\eta^2\text{-HC}(\text{PPh}_2)_3]\text{-Fe}(\text{CO})_3$ (**7**) with $[\text{Rh}(\text{CO})_2\text{Cl}]_2$ in THF to produce $\{(\text{CO})_3\text{Fe}[\mu\text{-}\eta^2\text{:}\eta^1\text{-HC}(\text{PPh}_2)_3]\text{Rh}(\text{CO})_2\}^+[\text{Rh}(\text{CO})_2\text{Cl}_2]^-$ (**8**),¹² whose X-ray structure indicated an Fe–Rh bond and an unsymmetric bridging $\text{HC}(\text{PPh}_2)_3$, the reaction being drawn in Scheme 3. The monodentate triphosphine **7** has a pentacoordinate Fe(0) center and a dangling PPh_2 , very similar to the monodentate dppm **1**. Therefore, it was thought worthwhile to react **1** with $[\text{Rh}(\text{CO})_2\text{Cl}]_2$. When compound **1** is allowed to react with $[\text{Rh}(\text{CO})_2\text{Cl}]_2$, interestingly $(\eta^5\text{-MeC}_5\text{H}_4)\text{Fe}(\mu\text{-CO})_2\text{-}(\mu\text{-}\eta^1\text{:}\eta^1\text{-dppm})\text{Rh}(\text{CO})_2$ (**9**) forms in 88% yields, instead of an imagined complex $[(\eta^4\text{-MeC}_5\text{H}_5)\text{Fe}(\text{CO})_2(\mu\text{-}\eta^1\text{:}\eta^1\text{-dppm})\text{Rh}(\text{CO})_2]^+[\text{Rh}(\text{CO})_2\text{Cl}_2]^-$ (Scheme 4). The immediately formed Fe–Rh heterobimetallic complex **9** sequentially sums up a PPh_2 ligation, an *endo*-H atom elimination, and post rearrangements in one treatment. The results here are completely different from the

(10) (a) Schmidbauer, H.; Wohlleben, A.; Wagner, F.; Orama, O.; Huttner, G. *Chem. Ber.* **1977**, *110*, 1748. (b) Briant, C. E.; Hall, K. P.; Mingos, D. M. P. *J. Chem. Soc., Chem. Commun.* **1983**, 843. (c) Uson, R.; Laguna, A.; Fornies, J.; Valenzuela, I.; Jones, P. G.; Sheldrick, G. M. *J. Organomet. Chem.* **1984**, *273*, 129. (d) Jones, P. G. *J. Organomet. Chem.* **1988**, *345*, 405. (e) Kim, H. P.; Fanwick, P. E.; Kubiak, C. P. *J. Organomet. Chem.* **1988**, *346*, C39. (f) Manojlovic-Muir, L.; Henderson, A. N.; Treurnicht, I.; Puddephatt, R. J. *Organometallics* **1989**, *8*, 2055. (g) Alvarez, S.; Rossell, O.; Seco, M.; Valls, J.; Pellinghelli, M. A.; Tiripicchio, A. *Organometallics* **1991**, *10*, 2309. (h) Stutzer, A.; Bissinger, P.; Schmidbauer, H. *Chem. Ber.* **1992**, *125*, 367. (i) Jones, P. G.; Thone, C. *Acta Cryst.* **1992**, *C48*, 1312. (j) Lin, I. J.-B.; Liu, C.-W.; Liu, L.-K.; Wen, Y.-S. *Organometallics* **1992**, *11*, 1447. (k) Braunstein, P.; Knorr, M.; Tiripicchio, A.; Camellini, M. T. *Inorg. Chem.* **1992**, *31*, 3685. (l) Balch, A. L.; Noll, B. C.; Olmstead, M. M.; Toronto, D. V. *Inorg. Chem.* **1992**, *31*, 5226. (m) Davila, R. M.; Elduque, A.; Grant, T.; Staples, R. J.; Fackler, J. P., Jr. *Inorg. Chem.* **1993**, *32*, 1749.

(11) (a) Fieser, L. F.; Fieser, M. *Reagents for Organic Synthesis*; Wiley: New York, 1967–70; Vol. 1, pp. 1256–1258; Vol. 2, p454; Vol. 3, p330. (b) Deeming, A. J.; Ullah, S. S.; Domingos, A. J. P.; Johnson, B. F. G.; Lewis, J. *J. Chem. Soc., Dalton Trans.* **1974**, 2093.

(12) Bahsoun, A. A.; Osborn, J. A.; Bird, P. H.; Nucciarone, D.; Peter, A. Av. *J. Chem. Soc., Chem. Commun.* **1984**, 72.

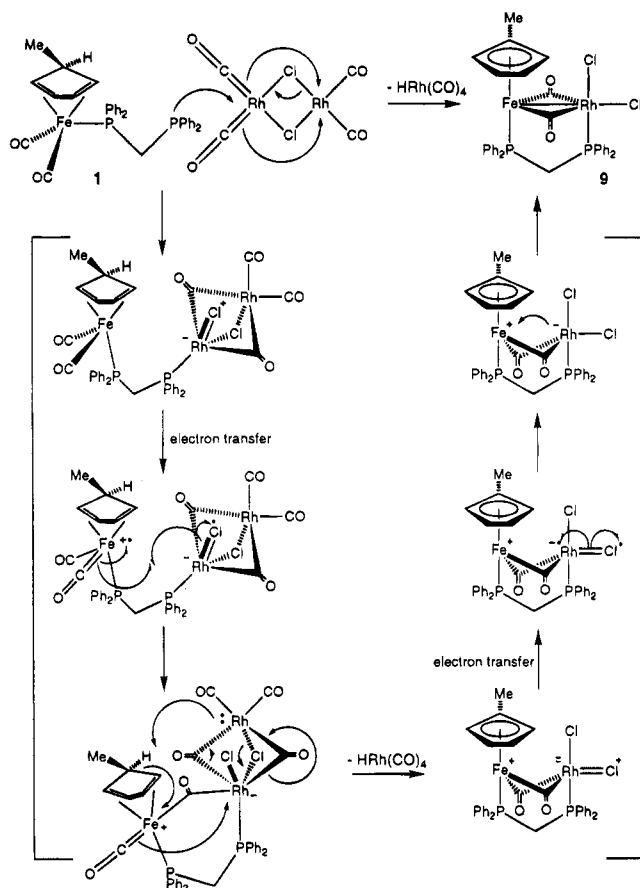
Scheme 4



general reaction of $[\text{Rh}(\text{CO})_2\text{Cl}]_2$ with a monodentate PR_3 : $[\text{Rh}(\text{CO})_2\text{Cl}]_2$ reacts with a variety of tertiary PR_3 ligands to give (halo)(carbonyl)(phosphine)rhodium complexes. Many confusing reports exist in the literature concerning the mechanism and intermediates involved. Depending on the molar ratio PR_3 to Rh, the final products could either the chloro-bridged dimer *cis/trans*- $[\text{RhCl}(\text{CO})\text{PR}_3]_2$ with a PR_3 to Rh ratio of one or *trans*- $\text{Rh}(\text{CO})_2(\text{PR}_3)_2$ with a PR_3 to Rh ratio greater than one.¹³ Complex **9** exhibits in the IR spectrum ν_{CO} bands at 1853 and 1809 cm^{-1} , indicating that only bridging carbonyl ligands are present. The characteristic pattern of 2:1:2 integration ratio for the $(\eta^4\text{-MeC}_5\text{H}_5)$ fragment of **1** disappears in the ^1H NMR spectrum of **9**, in which two new chemical shifts with equal intensity typical for a $(\eta^5\text{-MeC}_5\text{H}_4)$ moiety are observed at δ 4.86 (2H) and 4.43 (2H). The methylene H atoms of dppm and the methyl H atoms of $\eta^5\text{-MeC}_5\text{H}_4$ ring in **9** occur at δ 2.25 and 1.92, respectively. The methylene H resonance shows a substantial upfield shift from δ 3.0 in **1** whereas the methyl H resonance shows a substantial downfield shift from δ 0.27 in **1**. The methylene H atoms in **9** are apparently very different in local environment from the corresponding methylene H atoms in **6** which has also the $(\eta^5\text{-MeC}_5\text{H}_4)$ ring attached to Fe atom. Complex **9** exhibits in the ^{31}P NMR spectrum chemical shifts at δ 77.78 (d) and 47.03 (dd), the initial peaks at δ 66.38 and -25.60 in compound **1** being replaced completely. The ^{31}P peak pattern at δ 47.03 (dd) illustrates couplings to both Rh atom and the remaining P atom with $^1J_{\text{RhP}} = 127.2$ Hz and $^{2+3}J_{\text{PP}} = 71.8$ Hz. Shown in Figure 3 is the single-crystal X-ray structure of **9** which reveals in the solid state two crystallographically independent molecules per asymmetric unit. On the basis of the spectroscopic and crystallographic results, the molecular structure of complex **9** is found to realize the formation of an Fe–Rh bond and the change of the $\eta^4\text{-MeC}_5\text{H}_5$ bonding mode in **1** to $\eta^5\text{-MeC}_5\text{H}_4$ bonding in **9**. To the best of our knowledge, this is the first reported transformation from (cyclopentadiene)–Fe(O) to (cyclopentadienyl)–Fe(I) with simultaneous formation of an Fe–Rh bond.

The $(\eta^5\text{-C}_5\text{H}_5)\text{Fe}(\mu\text{-CO})_2(\mu\text{-}\eta^1:\eta^1\text{-dppm})\text{Rh}$ skeleton was reported by Shaw *et al.* in their treatment of $(\eta^5\text{-C}_5\text{H}_5)\text{Fe}(\text{CO})\text{C}(\text{O})\text{Me}(\eta^1\text{-dppm})$ with $[\text{Rh}(\text{CO})_2\text{Cl}]_2$ to give

Scheme 5



$(\eta^5\text{-C}_5\text{H}_5)\text{Fe}(\mu\text{-CO})_2(\mu\text{-}\eta^1:\eta^1\text{-dppm})\text{Rh}(\text{COMe})\text{Cl}$, whose slow decarbonylation in acetone deposited $(\eta^5\text{-C}_5\text{H}_5)\text{Fe}(\mu\text{-CO})_2(\mu\text{-}\eta^1:\eta^1\text{-dppm})\text{Rh}(\text{Me})\text{Cl}$ and $(\eta^5\text{-C}_5\text{H}_5)\text{Fe}(\mu\text{-CO})_2(\mu\text{-}\eta^1:\eta^1\text{-dppm})\text{RhCl}_2$ in the ratio 0.4:0.6.¹⁴

One of the possible mechanisms concerning the formation of an Fe–Rh complex is outlined in Scheme 5. Although detailed mechanistic studies are yet to pursue, the authors currently speculate that, after the monodentate dppm coordination to Rh atom, a single electron transfer step proceeds before the *endo*-H atom abstraction and the $\text{HRh}(\text{CO})_4$ extrusion. By stoichiometry, there would be 1 equiv of byproduct $\text{HRh}(\text{CO})_4$ which has not been isolated experimentally, partly because

(13) Hughes, R. P. In *Comprehensive Organometallic Chemistry*; Wilkinson, G., Stone, F. G. A., Abel, E. W., Eds.; Pergamon Press: Oxford, U.K., 1982; Vol. 5, pp 277–540.

(14) Shaw, B. L.; Smith, M. J.; Stretton, G. N.; Thornton-Pett, M. *J. Chem. Soc., Dalton Trans.* **1988**, 2099.

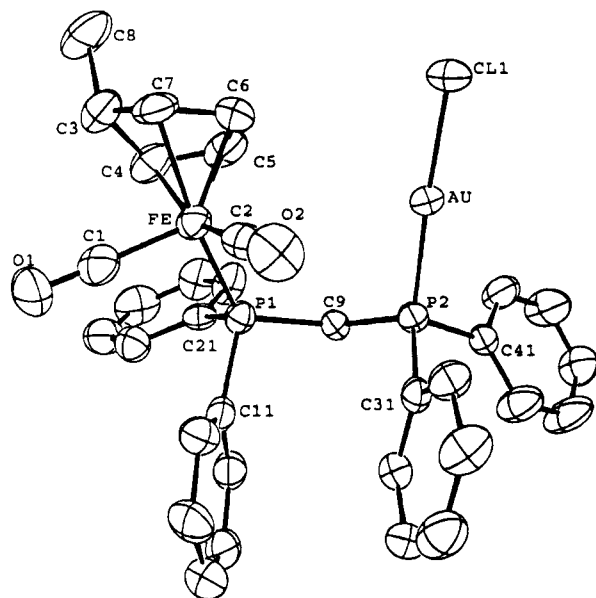
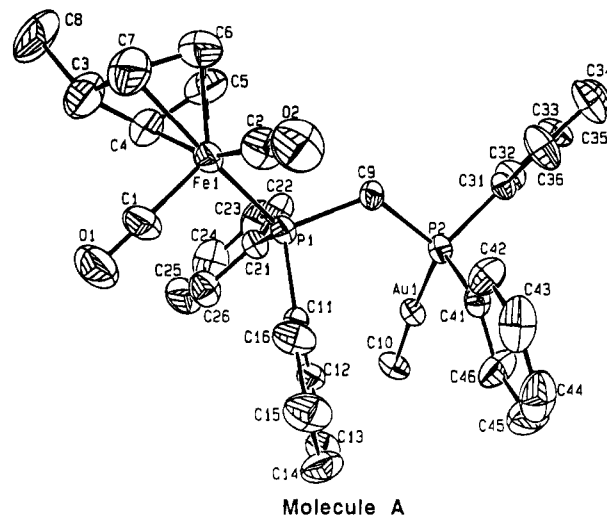


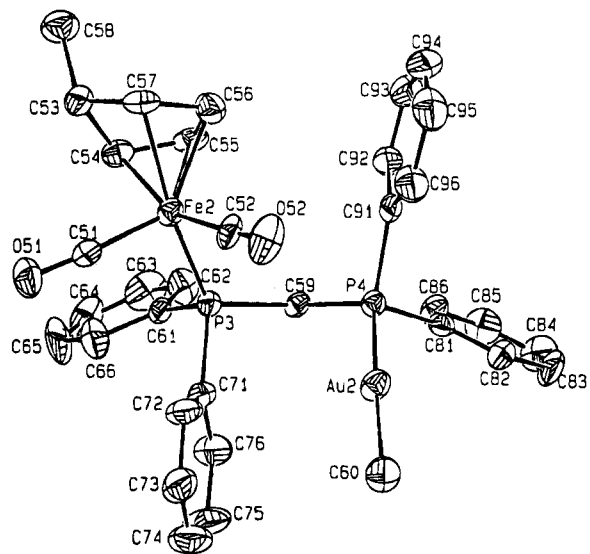
Figure 1. Molecular plot of complex **4** with the atomic numbering sequence. The thermal ellipsoids are drawn at the 50% level. The H atoms are omitted for clarity. Selected bond lengths (Å): Au–P2, 2.226(22); Au–Cl, 2.290(2); Fe–P1, 2.217(3); Fe–C1, 1.747(10); Fe–C2, 1.765(11); Fe–C4, 2.120(9); Fe–C5, 2.036(9); Fe–C6, 2.040(9); Fe–C7, 2.105(8); P1–C9, 1.855(8); P2–C9, 1.829(8); O1–C1, 1.158(12); O2–C2, 1.138(13). Selected bond angles (deg): P1–Fe–C1, 95.4(3); P1–Fe–C2, 96.6(3); C1–Fe–C2, 101.5(4); P2–Au–Cl, 176.44(8); P1–C9–P2, 120.4(4); Au–P2–C9, 112.4(3); Fe–P1–C9, 124.1(3).

HRh(CO)₄ aggregates quickly to clusters.¹⁵ Only spectroscopic evidence for rhodium clusters was obtained. The *endo*-H atom abstraction here could be viewed as an oxidative addition of the unique *endo*-C–H unit to Fe and Rh centers simultaneously with aromatization of cyclopentadiene ring as a driving force, eventually leading to the formation of an Fe–Rh bond. Such a speculation comes in passively because, in the Fe–Au heterobimetallic system, the monodentate dppm ligation to Au center followed by the *endo*-H atom elimination of the (η^4 -MeC₅H₅) ring using Ph₃C⁺PF₆[–] does not lead to an Fe–Au bond formation. The *endo*-H atom in the Fe–Rh system is likely eliminated in a manner different from being a hydride.

Crystallography. Complex **4** crystallizes with the occlusion of 1 mol of CH₂Cl₂ in the monoclinic space group P2₁/n. As shown in Figure 1, the X-ray structure of **4** gives no evidence of an Fe–Au bond [Fe···Au distance = 4.081(2) Å]. The two metal centers are only linked together by the dppm bridge. The Fe–P1–C9, P1–C9–P2, and Au–P2–C9 angles of 124.1(3), 120.4(5), and 112.4(3)°, respectively, result in the formation of a slightly distended W-shaped Fe–P1–C9–P2–Au fragment. The Cl atom is atop the Au atom [Au–Cl = 2.290(2) Å] from a near linear angle [\angle Cl–Au–P2 = 176.5(1)°]. The Fe–P1 length of 2.218(3) Å is similar to the those of closely related Fe–P bonds in the literature: for example 2.202(2) Å in (η^4 -MeC₅H₅)Fe(CO)₂(PMePh₂) and 2.208(1) Å in [(η^4 -MeC₅H₅)Fe(CO)₂]₂(μ -dppe).² The Au–P2 length of 2.226(2) Å is in



Molecule A



Molecule B

Figure 2. Molecular plot of complex **5** with atomic numbering sequence. The thermal ellipsoids are drawn at the 50% level. The H atoms are omitted for clarity. Selected bond lengths (Å): Au1–P2, 2.291(3); Au1–C10, 2.053(11); Fe1–P1, 2.212(3); Fe1–C1, 1.727(11); Fe1–C2, 1.732(14); Fe1–C4, 2.116(15); Fe1–C5, 2.021(13); Fe1–C6, 1.998(14); Fe1–C7, 2.099(15); P1–C9, 1.842(10); P2–C9, 1.849(10); Au2–P4, 2.284(3); Au2–C60, 2.112(10); Fe2–P3, 2.204(3); Fe2–C51, 1.735(11); Fe2–C52, 1.769(11); Fe–C54, 2.110(10); Fe2–C55, 2.057; Fe2–C56, 2.055; Fe2–C57, 2.076(9); P3–C59, 1.852(9); P4–C59, 1.810(10). Selected bond angles (deg): P2–Au1–C10, 177.3(4); P1–Fe1–C1, 97.1(4); P1–Fe1–C2, 95.1(5); Fe1–P1–C9, 113.5(4); P1–C9–P2, 121.5(6); Au1–P2–C9, 117.8(3); P4–Au2–C60, 175.1(3); P3–Fe2–C51, 96.5(3); P3–Fe2–C52, 95.2(3); Fe2–P3–C59, 120.7(3); P3–C59–P4, 118.4(5); Au2–P4–C59, 116.1(3).

agreement with the 2.238 Å found in (dppm)Au₂Cl₂¹⁶ and in [(dppm)₂Au₃Cl₂]⁺[Au(C₆H₅)₃Cl][–]¹⁷ but considerably shorter than the 2.391 Å found in (dppm)₃Au₄L₂.¹⁸ The ring Me group is *exo* on the cyclopentadiene from Fe. The coordination geometry around Fe may be

(16) Schmidbaur, H.; Wohlleben, A.; Wagner, F.; Orama, O.; Huttner, G. *Chem. Ber.* **1977**, *110*, 1748.

(17) Uson, R.; Laguna, A.; Laguna, M.; Fernandez, E.; Villacampa, M. D.; Jones, P. G.; Sheldrick, G. M. *J. Chem. Soc., Dalton Trans.* **1983**, 1679.

(18) van der Velden, J. W. A.; Bour, J. J.; Pet, R.; Bosman, W. P.; Noordik, J. H. *Inorg. Chem.* **1983**, *22*, 3112.

(15) (a) Vidal, J. L.; Walker, W. E. *Inorg. Chem.* **1981**, *20*, 249. (b) Vidal, J. L.; Schoening, R. C.; Walker, W. E. *A. C. S. Symp. Ser.*, **155** (*React. Met.-Met. Bonds*) 61–83, 1981.

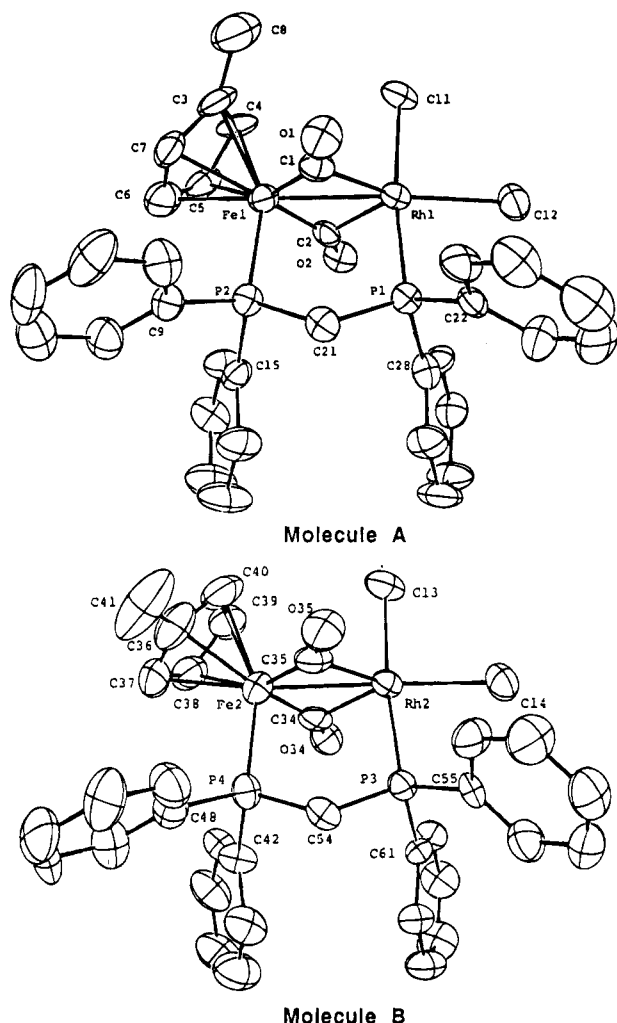


Figure 3. Molecular plots of complex **9** with atomic numbering sequence. The thermal ellipsoids are drawn at the 50% probability level. The H atoms are omitted for clarity. Selected bond lengths (Å): Rh1–Fe1, 2.611(2); Rh1–P1, 2.262(3); Rh1–C11, 2.390(3); Rh1–C12, 2.340(3); Rh1–C1, 2.057(9); Rh1–C2, 2.050(8); Rh2–Fe2, 2.613(2); Rh2–P3, 2.261(3); Rh2–C13, 2.396(3); Rh2–C14, 2.334(3); Rh2–C34, 2.049(9); Rh2–C35, 2.042(9); Fe1–P2, 2.211(3); Fe2–P4, 2.233(3). Selected bond angles (deg): Fe1–Rh1–P1, 94.59(7); Fe1–Rh1–C11, 92.25(8); Fe1–Rh1–C12, 173.30(8); P1–Rh1–C11, 173.14(9); P1–Rh1–C12, 84.56(9); P1–Rh1–C1, 88.8(3); P1–Rh1–C2, 92.9(2); C11–Rh1–C12, 88.72(9); C11–Rh1–C1, 95.7(3); C11–Rh1–C2, 92.5(2); C1–Rh1–C2, 88.2(4); Fe2–Rh2–P3, 94.44(7); Fe2–Rh2–C13, 92.19(8); Fe2–Rh2–C14, 177.18(9); P3–Rh2–C13, 173.3(1); P3–Rh2–C14, 85.68(9); P3–Rh2–C34, 92.4(2); P3–Rh2–C35, 89.0(3); C13–Rh2–C14, 87.7(1); C13–Rh2–C34, 91.9(2); C13–Rh2–C35, 96.2(3); C34–Rh2–C35, 88.5(4); Rh1–Fe1–P2, 96.40(8); P2–Fe1–C1, 90.2(3); P2–Fe1–C2, 92.3(3); C1–Fe1–C2, 102.7(4); Rh2–Fe2–P4, 96.44(8); P4–Fe2–C34, 91.3(3); P4–Fe2–C35, 91.3(3); C34–Fe2–C35, 102.1(4); Rh1–C1–Fe1, 84.1(4); Rh1–C2–Fe1, 84.5(4); Rh2–C34–Fe2, 84.6(4); Rh2–C35–Fe2, 84.4(4). Selected torsion angles (deg): P1–Rh1–Fe1–P2, –1.6(1); P3–Rh2–Fe2–P4, –2.4(1); Rh1–Fe1–centroid1–C3, –51.1(4); Rh2–Fe2–centroid2–C36, –108.8(5). Selected interplanar angles (deg): [Rh1, Fe1, C1, O1, C2, O2]–[Rh1, Fe1, P1, C11, C12], 93.4(1); [Rh2, Fe2, C34, O34, C35, O35]–[Rh2, Fe2, P3, C13, C14], 87.1(1).

described as a distorted square pyramid with one of the CO ligands at the apical position. The second CO ligand is in the basal plane *trans* to one of the double bonds, and the PPH₂CH₂– ligand is *trans* to the second double

bond. The diene atoms C4, C5, C6, and C7 are coplanar within 0.001(15) Å. The plane made up with C8, C3, Fe, C1, and O1 is planar to within 0.005(13) Å making an interplanar angle of 91.7(4)° with the plane of C4–C7. The apical CO ligand is seemingly farther away from the Fe core [Fe–C2 = 1.764(11) Å] than the basal CO [Fe–C1 = 1.746(10) Å].

Slow evaporation of a CH₂Cl₂/*n*-hexane solution of **5** gave crystals suitable for X-ray structure analysis revealing two crystallographically independent molecules. The structural parameters of **5** are similar to those of **4** except for the Me replacement of Cl and the distended W-shaped dppm on attachment of Fe and Au atoms. For **5**, the coordination geometry around the Fe atom may also be described as a distorted square pyramid, the same as in **4**. The diene atoms C4, C5, C6, and C7 and C54, C55, C56, and C57 are respectively coplanar to within 0.002(22) and 0.004(14) Å. The plane of C8, C3, Fe1, C1, O1 (deviations 0.0182 Å) and that of C58, C53, Fe2, C51, O51 (deviations 0.012 Å) are each perpendicular to the connecting diene planes C4–C7 and C54–C57, with interplanar angles of 89.3(5) and 87.8(4)°, respectively. That is, the planar diene skeleton is orthogonal to the plane made up of the *exo*-C atom, the unique C atom of the cyclopentadiene ring, Fe, and the apical CO ligand. The X-ray structure gives no evidence of a direct Fe–Au bond, Fe···Au distances being 6.300(2) and 4.916(2) Å for the two independent molecules. The two metals are simply linked by dppm. The Au–P lengths are considerably elongated compared to the corresponding values in the Au–Cl analog. The structural parameters obtained for the two crystallographically independent molecules are very similar except the torsion angles Fe1–P1···P2–Au1 = –158.1(2)° and Fe2–P3···P4–Au2 = 90.8(1)°.

Shown in Figure 3 are the ORTEP molecular drawings of the Fe–Rh heterobimetallic complex **9**. The complex reveals, in the solid state X-ray structure, two CO bridges and a direct Fe–Rh bond in addition to the dppm bridge, the five-membered ring Fe–P–C–P–Rh being approximately orthogonal to the plane made of CO bridges. Crystallized in the monoclinic space group *P2₁/a* with 8 molecules per unit cell, complex **9** gives two crystallographically independent molecules that are similar in structural parameters and different only in the orientation of the ring Me group with respect to Fe–Rh bond. The torsion angles of C3–Fe1–Rh1–C11 and C36–Fe2–Rh2–C13 are –30.2(2) and –55.5(3)°, respectively, and the torsion angles of C3–centroid1–Fe1–Rh1 and C36–centroid2–Fe2–Rh2 are 146.9(6) and 140.5(7)°, respectively, where centroid1 and centroid2 are the centers of gravity of the respective rings. The distances of Fe–Rh are 2.611(2) and 2.613(2) Å for the two molecules. Such bond lengths are shorter than the reported 2.699(4) Å in Fe(CO)₄(*μ*-dppm)RhCl(CO),¹⁹ 2.762(2) Å in (CO)₂Fe(*μ*-CO)(*μ*-C₇H₇)Rh(dppe),²⁰ and 2.776 Å in 8¹³ but longer than 2.557(2) Å in (C₄H₄)(CO)₃–FeRh(*η*⁵-C₅H₅).²¹ The average Rh–CO and Fe–CO bond distances are 2.049 and 1.832 Å, respectively,

(19) Jacobsen, G. B.; Shaw, B. L.; Thomson-Pett, M. *J. Chem. Soc., Chem. Commun.* **1986**, 13.

(20) Ball, R. G.; Edelmann, F.; Kiel, G.-Y.; Takats, J.; Drews, R. *Organometallics* **1986**, *5*, 829.

(21) King, M.; Holt, E. M.; Radnia, P.; McKennis, J. S. *Organometallics* **1982**, *1*, 1718.

Table 1. Final Fractional Coordinates and B Values (Å²) for Non-H Atoms of Complex 4, (η^4 -MeC₅H₅)Fe(CO)₂(μ - η^1 : η^1 -dppm)AuCl-CH₂Cl₂

atom	x	y	z	B _{iso}	atom	x	y	z	B _{iso}
Au	0.93956(3)	0.08920(1)	0.03346(2)	2.88(2)	C15	1.3076(9)	0.3063(4)	0.3458(6)	4.0(5)
Fe	1.06755(12)	0.05617(5)	0.30102(7)	3.04(5)	C16	1.3127(9)	0.2436(4)	0.3171(5)	3.6(4)
P1	1.2058(2)	0.1240(1)	0.2663(1)	2.7(1)	C21	1.3662(7)	0.0946(4)	0.3072(5)	2.9(4)
P2	1.0752(2)	0.1688(1)	0.0683(1)	2.7(1)	C22	1.4204(9)	0.1023(4)	0.3979(6)	4.2(5)
Cl1	0.7918(2)	0.0116(1)	-0.0079(2)	4.3(1)	C23	1.5350(11)	0.0745(5)	0.4331(7)	5.6(6)
Cl2	0.5303(4)	0.2061(2)	0.1088(3)	10.2(2)	C24	1.5966(10)	0.0391(5)	0.3807(8)	6.0(6)
Cl3	0.4790(3)	0.0847(2)	0.0254(2)	8.2(2)	C25	1.5430(10)	0.0302(5)	0.2911(7)	5.1(5)
O1	1.1179(8)	0.0855(3)	0.4916(4)	6.4(4)	C26	1.4284(9)	0.0580(5)	0.2557(6)	4.4(5)
O2	0.8420(7)	0.1299(3)	0.2375(4)	5.4(4)	C31	1.0070(8)	0.2407(4)	0.1038(5)	2.7(4)
C1	1.0967(9)	0.0754(4)	0.4151(6)	3.9(4)	C32	0.8776(8)	0.2465(4)	0.0834(6)	3.4(4)
C2	0.9329(9)	0.1022(4)	0.2591(6)	3.7(4)	C33	0.8205(9)	0.3031(4)	0.0994(6)	4.5(5)
C3	1.0890(10)	-0.0592(4)	0.3753(6)	4.4(5)	C34	0.8930(11)	0.3536(4)	0.1375(6)	4.7(5)
C4	1.1812(9)	-0.0260(4)	0.3296(6)	4.2(5)	C35	1.0209(11)	0.3475(4)	0.1595(6)	4.4(5)
C5	1.1264(11)	-0.0199(4)	0.2381(7)	4.7(5)	C36	1.0786(8)	0.2917(4)	0.1422(5)	3.5(4)
C6	0.9959(11)	-0.0214(4)	0.2278(6)	4.8(5)	C41	1.1400(8)	0.1938(4)	-0.0276(5)	2.9(4)
C7	0.9737(9)	-0.0290(4)	0.3175(6)	4.1(4)	C42	1.1777(11)	0.1490(4)	-0.0808(6)	4.9(5)
C8	1.0879(12)	-0.1324(4)	0.3729(7)	6.5(6)	C43	1.2268(12)	0.1660(5)	-0.1544(7)	6.2(6)
C9	1.2158(7)	0.1454(4)	0.1497(5)	2.7(3)	C44	1.2400(10)	0.2275(5)	-0.1752(6)	5.0(5)
C11	1.2112(8)	0.2036(4)	0.3166(5)	2.9(4)	C45	1.1986(13)	0.2731(5)	-0.1249(7)	6.5(7)
C12	1.1092(8)	0.2263(4)	0.3485(5)	3.6(4)	C46	1.1486(11)	0.2566(4)	-0.0512(6)	5.5(6)
C13	1.1055(10)	0.2890(4)	0.3771(6)	4.4(5)	C50	0.5861(10)	0.1316(6)	0.0898(7)	6.3(6)
C14	1.2037(11)	0.3291(4)	0.3731(6)	4.7(5)					

whereas the average bond angles of Rh–C–O and Fe–C–O are 124.3 and 150.9°, respectively, indicative of the semibridging nature of CO ligands. The two Cl ligands coordinated to Rh are *cis*, one *trans* to Fe and the other *trans* to P. Rh1, Fe1, Cl1, Cl2, and P1 are coplanar (± 0.109 Å). So are Rh2, Fe2, Cl3, Cl4, and P2 (± 0.076 Å). The Cp rings C3–C8 and C36–C41 are respectively planar (to within 0.0046 and 0.064 Å), with coordinated Fe atoms displaced by 1.739(5) and 1.737(6) Å. The overall bonding geometry around Fe could be described as an octahedron with a dative bond toward Rh which partially returns electron density *via* the semibridging CO ligands. In the solid state, there are 2 CH₂Cl₂ solvate molecules for each Fe–Rh complex.

Experimental Section

General Methods. All manipulations were performed under an atmosphere of prepurified nitrogen with standard Schlenk techniques. All solvents were distilled from an appropriate drying agent.²² Infrared spectra were recorded in CH₂Cl₂ using CaF₂ optics on a Perkin-Elmer 882 spectrophotometer. The ¹H NMR and ¹³C NMR spectra were obtained on Bruker AC200/AC300 spectrometers, with chemical shifts reported in δ values relative to the residual solvent resonance of CDCl₃ (¹H 7.24 ppm, ¹³C 77.0 ppm). The ³¹P{¹H} NMR spectra were obtained on Bruker AC200/AC300 spectrometers using 85% H₃PO₄ as an external standard (0.00 ppm). The melting points (uncorrected) were determined on a Yanaco MPL melting-point apparatus. Compound 1³ and (η^5 -C₅H₅)Fe(CO)₃I²³ were prepared according to the literature procedure. Other reagents were obtained from commercial sources e.g. Aldrich, Merck, and used without further purification.

Synthesis of (η^4 -MeC₅H₅)Fe(CO)₂(μ - η^1 : η^1 -dppm)AuCl (4). (C₄H₉S)AuCl (0.278 g, 0.868 mmol) and (η^4 -MeC₅H₅)Fe(CO)₂(η^1 -dppm) (0.50 g, 0.868 mmol) were placed in a flask and cooled to -30 °C. THF (30 mL) also cooled to -30 °C was transferred into the reaction flask *via* cannula. The reaction mixture was stirred at -30 °C for 30 min before being warmed up to room temperature and stirred overnight. The mixture was then filtered through a pad of Celite and the

solvent removed on a rotary evaporator. The resultant greenish-yellow solids were prepared for chromatography on a column of nonactivated alumina, eluting with 1:4 ethyl acetate/*n*-hexane to obtain one yellow band. The yellow solution was collected which, after solvent removal, gave yellow, powdery 4 (0.482 g, 68.7%). Crystals suitable for X-ray crystallography were grown from a CH₂Cl₂/*n*-hexane mixture by slow evaporation. 4: mp 103–105 °C; IR (CH₂Cl₂) ν_{CO} 1966 (vs), 1906 (vs) cm⁻¹; ³¹P NMR (CDCl₃) δ 65.78 (s), 19.04 (s); ¹H NMR (CDCl₃) δ 7.50–7.31 (m, 20H, Ph), 4.87 (s, 2H, -CH=CHCHMe), 3.39 (b, 2H, PCH₂P), 2.56 (s, 1H, -CH=CHCHMe), 2.27 (s, 2H, CH=CHCHMe), 0.26 (d, 3H, ⁵J_{PH} = 9 Hz, Me); ¹³C NMR (CDCl₃) δ 219.3 (s, CO), 133.7–128.6 (m, Ph), 82.3 (s, -CH=CHCHMe), 58.4 (s, -CH=CHCHMe), 51.1 (s, -CH=CHCHMe), 32.2 (s, PCH₂P), 28.1 (s, Me); MS (FAB) *m/z* 774 (M⁺ - Cl). Anal. Calcd for C₃₃H₃₀AuClFeO₂P₂: C, 48.99; H, 3.74. Found: C, 48.49; H, 3.92.

Reaction of 4 with MeLi. Complex 4 (0.194 g, 0.240 mmol) was dissolved in dry THF (20.0 mL) and cooled to -78 °C. Excess MeLi (1.0 mL, 1.6 M in ether) diluted in ether (10.0 mL) and kept at -78 °C was dropwise added to the stirring solution over a period of 10 min. The mixture was stirred at -78 °C for 1 h and gradually warmed up to room temperature with continued stirring for a further 3 h. The solution was then filtered on a glass frit through a short plug of alumina. The resultant clear yellow solution gave a yellow powdery material after solvent removal on a rotary evaporator. The solid material was redissolved in a minimum amount of CH₂Cl₂ and applied to the top of a column of alumina. The column was eluted with 10% ethyl acetate in *n*-hexane to yield a bright yellow solid of (η^4 -MeC₅H₅)Fe(CO)₂(μ - η^1 : η^1 -dppm)AuMe (5) (0.14 g, 74.0%) after solvent removal. Crystals suitable for X-ray crystallography were grown from a mixture of CH₂Cl₂/*n*-hexane by slow evaporation. 5: mp 141–142 °C; IR (CH₂Cl₂) ν_{CO} 1962 (vs), 1902 (vs) cm⁻¹; ³¹P NMR (CDCl₃) δ 65.36 (s), 34.30 (s); ¹H NMR (CDCl₃) δ 7.61–6.96 (m, 20H, Ph), 4.86 (s, 2H, -CH=CHCHMe-), 3.37–3.32 (m, 2H, PCH₂P), 2.59 (b, 1H, -CH=CHCHMe-), 2.28 (s, 2H, -CH=CHCHMe-), 0.27 (d, ⁴J_{PH} = 9 Hz, 3H, Me-), 0.02 (d, ³J_{PH} = 8.1 Hz, 3H, AuMe); ¹³C NMR (CDCl₃) δ 1.02 (s, AuMe), 28.16 (s, Me), 30.35 (s, PCH₂P), 51.08 (s, -CH=CHCHMe-), 58.12 (s, -CH=CHCHMe-), 82.22 (s, -CH=CHCHMe-), 134.5–125.5 (m, Ph), 219.4 (b, CO); MS (FAB) *m/z* 775 (M⁺ - Me). Anal. Calcd for C₃₄H₃₃AuFeO₂P₂: C, 51.78; H, 4.23. Found: C, 52.22; H, 4.53.

Synthesis of [(η^5 -MeC₅H₄)Fe(CO)₂(μ - η^1 : η^1 -dppm)AuCl]⁻PF₆⁻ (6). Complex 4 (0.80 g, 0.989 mmol) dissolved in CH₂-

(22) Perrin, D. D.; Armarego, W. L. F.; Perrin, D. R. *Purification of Laboratory Chemicals*; Pergamon Press: Oxford, U.K., 1981.

(23) (a) Dombek, B. D.; Angelici, R. J. *Inorg. Chim. Acta* **1973**, *7*, 345. (b) Meyer, T. J.; Johnson, E. C.; Winterton, N. *Inorg. Chem.* **1971**, *10*, 1673. (c) *Inorg. Synth.* **1971**, *12*, 36. (d) *Inorg. Synth.* **1963**, *7*, 110.

Table 2. Final Fractional Coordinates and B Values (Å²) for Non-H Atoms of Complex 5, (η^4 -MeC₅H₅)Fe(CO)₂(μ - η^1 : η^1 -dppm)AuMe

atom	x	y	z	B _{iso}	atom	x	y	z	B _{iso}
Au1	0.13000(3)	0.49479(2)	0.07305(2)	3.90(2)	C41	0.2275(6)	0.6620(6)	0.1064(5)	4.2(6)
Au2	0.71292(3)	0.68954(2)	0.22459(2)	4.18(2)	C42	0.2756(7)	0.7163(7)	0.1407(5)	5.7(6)
Fe1	0.40996(9)	0.50225(9)	0.31310(7)	4.43(8)	C43	0.3165(7)	0.7676(7)	0.1106(7)	7.6(8)
Fe2	0.54586(8)	0.90630(8)	0.14703(7)	3.34(7)	C44	0.3097(8)	0.7650(7)	0.0471(7)	8.2(9)
P1	0.3267(2)	0.5031(2)	0.2206(1)	3.7(1)	C45	0.2611(10)	0.7139(8)	0.0130(7)	8.7(9)
P2	0.1723(2)	0.5901(2)	0.1411(1)	3.7(1)	C46	0.2214(8)	0.6610(7)	0.0421(6)	6.7(7)
P3	0.6767(2)	0.8891(1)	0.1447(1)	3.2(1)	C51	0.5106(6)	0.8951(6)	0.0669(5)	4.1(5)
P4	0.7392(2)	0.8028(2)	0.2706(1)	3.2(1)	C52	0.5298(6)	0.8166(6)	0.1752(5)	4.2(5)
O1	0.5524(5)	0.4413(6)	0.2725(5)	9.8(7)	C53	0.4458(6)	1.0223(6)	0.1264(5)	4.5(5)
O2	0.4468(6)	0.6573(5)	0.3146(5)	10.5(7)	C54	0.5400(6)	1.0225(5)	0.1387(5)	4.4(6)
O51	0.4856(5)	0.8919(5)	0.0128(3)	6.8(5)	C55	0.5675(6)	1.0004(6)	0.2009(5)	4.7(6)
O52	0.5118(4)	0.7606(4)	0.1926(4)	6.4(5)	C56	0.5066(6)	0.9577(6)	0.2208(5)	4.5(6)
C1	0.4940(7)	0.4650(7)	0.2878(6)	6.7(8)	C57	0.4418(6)	0.9570(6)	0.1677(5)	4.0(5)
C2	0.4287(8)	0.5965(7)	0.3144(7)	7.5(8)	C58	0.4062(7)	1.0921(6)	0.1452(6)	6.1(7)
C3	0.4529(10)	0.3934(9)	0.3966(7)	9.6(10)	C59	0.7525(5)	0.8783(5)	0.2184(5)	3.2(5)
C4	0.3791(8)	0.3971(8)	0.3447(7)	7.9(8)	C60	0.6994(7)	0.5828(6)	0.1844(5)	5.2(6)
C5	0.3286(8)	0.4533(8)	0.3589(6)	7.6(9)	C61	0.7220(6)	0.9672(6)	0.1100(5)	3.8(5)
C6	0.3782(9)	0.5058(9)	0.3978(7)	9.3(10)	C62	0.7683(7)	1.0212(6)	0.1446(6)	5.6(7)
C7	0.4617(8)	0.4780(10)	0.4069(7)	10.1(11)	C63	0.7978(8)	1.0801(7)	0.1159(7)	8.1(9)
C8	0.4507(12)	0.3459(11)	0.4554(8)	14.4(15)	C64	0.7825(7)	1.0870(8)	0.0524(7)	8.4(9)
C9	0.2400(6)	0.5676(5)	0.2166(5)	3.9(5)	C65	0.7339(8)	1.0359(9)	0.0164(6)	8.5(9)
C10	0.0892(6)	0.4129(6)	0.0092(6)	5.2(6)	C66	0.7040(7)	0.9751(7)	0.0451(6)	6.5(7)
C11	0.3707(6)	0.5252(5)	0.1514(5)	3.8(5)	C71	0.7030(6)	0.8116(6)	0.0978(5)	4.4(5)
C12	0.3410(6)	0.4976(6)	0.0917(5)	4.5(6)	C72	0.6465(6)	0.7588(6)	0.0732(6)	5.1(6)
C13	0.3752(7)	0.5174(7)	0.0396(6)	6.4(7)	C73	0.6683(7)	0.7008(7)	0.0389(6)	6.5(7)
C14	0.4395(8)	0.5666(7)	0.0473(6)	6.9(8)	C74	0.7447(8)	0.6962(8)	0.0264(6)	7.9(8)
C15	0.4684(8)	0.5940(8)	0.1053(7)	7.8(8)	C75	0.8032(8)	0.7472(8)	0.0489(7)	8.9(9)
C16	0.4363(7)	0.5746(7)	0.1574(6)	5.9(7)	C76	0.7814(6)	0.8052(7)	0.0860(6)	6.2(7)
C21	0.2791(5)	0.4139(5)	0.1999(5)	3.6(5)	C81	0.8371(5)	0.8009(6)	0.3252(4)	3.6(5)
C22	0.2013(6)	0.3955(6)	0.2094(5)	4.9(6)	C82	0.8618(7)	0.7356(6)	0.3548(5)	5.2(6)
C23	0.1671(7)	0.3251(7)	0.1966(6)	7.0(7)	C83	0.9354(8)	0.7343(7)	0.3976(6)	7.1(7)
C24	0.2130(8)	0.2735(7)	0.1736(7)	7.9(8)	C84	0.9824(7)	0.7948(8)	0.4093(6)	7.5(8)
C25	0.2904(9)	0.2891(7)	0.1650(7)	7.5(8)	C85	0.9605(7)	0.8596(7)	0.3807(6)	6.5(7)
C26	0.3234(7)	0.3585(6)	0.1776(6)	5.9(7)	C86	0.8863(6)	0.8638(6)	0.3389(5)	4.7(6)
C31	0.0845(6)	0.6347(5)	0.1671(5)	3.6(5)	C91	0.6704(5)	0.8380(6)	0.3205(4)	3.6(5)
C32	0.0123(7)	0.5994(6)	0.1580(6)	5.3(6)	C92	0.6816(7)	0.9062(6)	0.3478(5)	5.0(6)
C33	-0.0559(7)	0.6319(7)	0.1762(6)	6.0(7)	C93	0.6332(7)	0.9298(7)	0.3895(6)	6.1(7)
C34	-0.0499(7)	0.6976(7)	0.2040(6)	6.6(7)	C94	0.5709(7)	0.8853(8)	0.3996(6)	7.5(8)
C35	0.0230(8)	0.7335(7)	0.2149(7)	7.5(9)	C95	0.5588(7)	0.8156(8)	0.3736(6)	6.8(8)
C36	0.0912(7)	0.7024(7)	0.1969(7)	7.2(8)	C96	0.6096(6)	0.7930(7)	0.3331(5)	5.5(7)

Cl₂ (15 mL) was treated with Ph₃C⁺PF₆⁻ (0.384 g, 0.989 mmol) in CH₂Cl₂ (15 mL) at 0 °C. The reaction mixture was stirred at 0 °C for 30 min before being gradually warmed up to room temperature and was stirred for a further 2.5 h. The solution was then filtered on a pad of Celite. The solvent was reduced to a small volume on a rotary evaporator. After the addition of anhydrous Et₂O, complex **6** precipitated as a light green solid material which was collected by filtration and recrystallized from CH₃CN (yield: 0.811 g, 86.0%). **6**: mp 160–162 °C; IR (CH₂Cl₂) ν_{CO} 2050 (vs), 2007 (vs) cm⁻¹; ³¹P NMR (CDCl₃) δ 56.48 (s), 20.68 (s), -143.38 (sept, ¹J_{PF} = 711 Hz); ¹H NMR (CDCl₃) δ 7.80–7.45 (m, 20H, Ph), 4.90 (s, 2H, Cp'- β), 4.87 (s, 2H, Cp'- α), 4.01 (m, 2H, PCH₂P), 1.83 (s, 3H, Me); ¹³C NMR (CDCl₃) δ 218.22 (s, CO), 133.86–129.70 (m, Ph), 107.36 (s, Cp' ipso), 89.01 (s, Cp'- β), 87.39 (s, Cp'- α), 31.57 (s, PCH₂P), 22.64 (s, Me); MS (FAB) *m/z* 808 (M⁺ - PF₆). Anal. Calcd for C₃₃H₂₉AuClF₆O₂P₃: C, 41.59; H, 3.07. Found: C, 41.65; H, 3.36.

Reaction of Compound 1 and [Rh(CO)₂Cl]₂. Compound **1** (0.115 g, 0.2 mmol) and [Rh(CO)₂Cl]₂ (0.085 g, 0.2 mmol) were dissolved in 15 mL of THF/30 mL of *n*-hexane. The color of solution changed gradually from yellow to red when red precipitates appeared in 10 min. The mixture was stirred for an additional 1 h, and then the solution was cannula transferred. The precipitate was washed with *n*-hexane (30 mL \times 3) to give red (η^5 -MeC₅H₄)Fe(μ -CO)₂(μ - η^1 : η^1 -dppm)RhCl₂ (**9**) (0.088 g, 88%). **9**: mp 189–190 °C (dec); IR (CH₂Cl₂) ν_{CO} 1854 (w), 1809 (s) cm⁻¹; ³¹P NMR (CDCl₃) δ 77.78 (d, ²J_{PP} = 71.8 Hz), 47.03 (dd, ²J_{PP} = 71.8 Hz, ¹J_{RhP} = 127.2 Hz); ¹H NMR (CDCl₃) δ 1.92 (b, 3H, Me), 2.25 (b, 2H, Ph₂PCH₂PPh₂), 4.43 (b, 2H, Cp'- α), 4.86 (b, 2H, Cp'- β), 7.19–7.47 (m, 20H, Ph); ¹³C NMR (CDCl₃) δ 12.0 (s, Me), 28.6 (m, Ph₂PCH₂PPh₂), 53.4 (s,

Cp'- α), 77.2 (s, Cp'- β), 88.6 (s, Cp'-*ipso*), 128.2–133.2 (m, Ph), 219.8 (dd, CO, ²J_{PC} = 14.2 Hz, ⁴J_{PC} = 1.85 Hz); MS (*m/z*) 767 (M⁺). Anal. Calcd for C₃₅H₃₃Cl₆FeO₂P₂Rh: C, 44.85; H, 3.55. Found: C, 45.22; H, 3.61.

X-ray Structure Analyses of Complexes 4, 5, and 9. Diffraction intensities were measured with background counts made for half the total scan time on each side of peak. Three standard reflections, remeasured after every 1 h, showed no significant decrease in intensity during data collection. Data were corrected for Lorentz–polarization and absorption (empirical ψ corrections). The structure was solved by direct methods with MULTAN.²⁴ Calculations and full matrix least-squares refinements were performed utilizing the NRCVAX program package.²⁵ All non-H atoms were refined with anisotropic thermal parameters with all hydrogen atoms idealized (C–H = 1.00 Å). Scattering factor curves of Fe, P, O, C, and H were taken from the ref 26. Final fractional coordinates of complexes **4**, **5**, and **9**, respectively, are given in Tables 1–3. Relevant structural parameters are listed in the captions of Figures 1–3, the molecular plots of complexes **4**, **5**, and **9**, respectively.

(24) Main, P. In *Crystallographic Computing 3: Data Collection, Structure Determination, Proteins and Database*; Sheldrick, G. M., Krueger, C., Goddard, R., Eds.; Clarendon: Oxford, U.K., 1985; pp. 206–215.

(25) Gabe, E. J.; Le Page, Y.; Lee, F. L. In *Crystallographic Computing 3: Data Collection, Structure Determination, Proteins and Database*; Sheldrick, G. M., Krueger, C., Goddard, R., Eds.; Clarendon: Oxford, U.K., 1985; pp. 167–174.

(26) Ibers, J. A.; Hamilton, W. C., Eds. *International Tables for X-ray Crystallography*; Kynoch: Birmingham, U.K. (current distributor D. Reidel, Dordrecht, The Netherlands), 1974; Vol. 4, Tables 2.2A and 2.3.1D.

Table 3. Final Fractional Coordinates and B Values (Å²) for Non-H Atoms of Complex 9, (η^5 -MeC₅H₄)Fe(μ -CO)₂(μ - η^1 : η^1 -dppm)RhCl₂·2CH₂Cl₂

atom	<i>x</i>	<i>y</i>	<i>z</i>	<i>B</i> _{iso}	atom	<i>x</i>	<i>y</i>	<i>z</i>	<i>B</i> _{iso}
Rh1	0.53935(4)	0.27155(4)	0.46664(3)	2.67(4)	C26	0.3397(6)	0.0606(6)	0.3373(5)	5.8(7)
Rh2	-0.04770(4)	0.23217(4)	0.97577(3)	2.91(4)	C27	0.3531(6)	0.1327(5)	0.3576(4)	4.7(6)
Fe1	0.54925(8)	0.32864(7)	0.56864(6)	2.88(7)	C28	0.3440(5)	0.2926(5)	0.3959(4)	3.0(5)
Fe2	0.03488(8)	0.17328(8)	0.10757(6)	3.41(8)	C29	0.3640(5)	0.3502(5)	0.3680(4)	3.1(5)
P1	0.41580(14)	0.23576(13)	0.44587(11)	2.74(12)	C30	0.3088(6)	0.3948(5)	0.3308(4)	4.0(5)
P2	0.42937(15)	0.30593(13)	0.56367(11)	2.83(14)	C31	0.2328(6)	0.3821(6)	0.3219(5)	5.1(6)
P3	0.05487(14)	0.26103(13)	0.94813(11)	2.80(12)	C32	0.2100(5)	0.3237(6)	0.3487(5)	5.0(7)
P4	0.14874(15)	0.18775(14)	0.106285(11)	3.18(14)	C33	0.2656(6)	0.2801(5)	0.3851(4)	4.3(6)
Cl1	0.66959(14)	0.30201(13)	0.47801(12)	3.94(14)	C34	-0.0053(5)	0.1316(5)	1.0028(4)	3.3(5)
Cl2	0.52366(15)	0.23295(15)	0.37021(11)	4.28(14)	C35	0.0109(5)	0.2687(5)	1.0590(4)	3.7(5)
Cl3	-0.16550(15)	0.20643(14)	0.99393(13)	4.73(16)	C36	0.0479(7)	0.1856(6)	1.1659(4)	6.0(7)
Cl4	-0.12205(15)	0.27922(16)	0.88428(12)	4.84(15)	C37	0.0859(6)	0.1234(7)	1.1575(5)	6.0(7)
O1	0.5770(4)	0.1739(3)	0.5668(3)	4.5(4)	C38	0.0306(6)	0.0768(6)	1.1201(5)	5.0(6)
O2	0.5024(3)	0.4220(3)	0.4648(3)	3.4(3)	C39	-0.0394(6)	0.1091(6)	1.1061(5)	5.3(7)
O34	-0.0209(4)	0.0801(3)	0.9721(3)	4.0(4)	C40	-0.0304(7)	0.1760(6)	1.1335(5)	6.1(8)
O35	0.0106(4)	0.3290(3)	1.0748(3)	5.1(4)	C41	0.0802(10)	0.2462(9)	1.2063(5)	11.3(12)
C1	0.5620(5)	0.2343(5)	0.5517(4)	3.1(5)	C42	0.1891(5)	0.1134(5)	1.0332(4)	3.4(5)
C2	0.5183(5)	0.3706(5)	0.4956(4)	2.6(5)	C43	0.1619(6)	0.0431(5)	1.0350(4)	4.2(6)
C3	0.6612(5)	0.3251(5)	0.6336(4)	4.4(5)	C44	0.1957(6)	-0.0134(5)	1.0167(5)	5.7(7)
C4	0.6536(5)	0.3877(5)	0.5989(4)	4.0(5)	C45	0.2559(7)	-0.0017(6)	0.9952(6)	6.8(8)
C5	0.5933(6)	0.4287(5)	0.6064(4)	4.2(6)	C46	0.2813(7)	0.0664(6)	0.9919(6)	6.7(8)
C6	0.5641(6)	0.3899(5)	0.6440(4)	4.5(6)	C47	0.2494(6)	0.1239(5)	1.0125(5)	4.9(7)
C7	0.6052(6)	0.3257(5)	0.6606(4)	4.1(6)	C48	0.2295(6)	0.2142(5)	1.1274(4)	3.9(5)
C8	0.7224(7)	0.2681(7)	0.6434(5)	7.2(8)	C49	0.2847(6)	0.1637(6)	1.1570(5)	5.5(7)
C9	0.4228(5)	0.2756(5)	0.6338(4)	3.2(5)	C50	0.3457(7)	0.1852(7)	1.2069(5)	6.6(7)
C10	0.3945(6)	0.3201(6)	0.6686(4)	4.5(6)	C51	0.3515(7)	0.2542(7)	1.2266(4)	6.9(8)
C11	0.3962(7)	0.2977(6)	0.7242(5)	5.5(7)	C52	0.2971(7)	0.3040(6)	1.1970(5)	6.4(8)
C12	0.4243(7)	0.2328(7)	0.7454(4)	6.3(7)	C53	0.2364(6)	0.2842(6)	1.1481(4)	5.2(6)
C13	0.4520(7)	0.1879(6)	0.7125(5)	6.2(7)	C54	0.1431(5)	0.2625(5)	1.0116(4)	3.0(5)
C14	0.4520(6)	0.2095(5)	0.6571(4)	4.5(6)	C55	0.0534(5)	0.3517(5)	0.9200(4)	2.9(5)
C15	0.3581(5)	0.3773(5)	0.5405(4)	3.1(5)	C56	0.0659(6)	0.3682(5)	0.8683(5)	4.4(6)
C16	0.3814(5)	0.4479(5)	0.5408(4)	3.7(6)	C57	0.0667(7)	0.4390(6)	0.8497(5)	5.5(7)
C17	0.3269(6)	0.5023(5)	0.5276(5)	4.7(7)	C58	0.0523(6)	0.4932(5)	0.8828(5)	5.3(7)
C18	0.2505(6)	0.4862(6)	0.5145(5)	5.5(7)	C59	0.0393(7)	0.4787(5)	0.9341(5)	5.6(7)
C19	0.2268(6)	0.4168(6)	0.5132(6)	6.0(8)	C60	0.0380(6)	0.4079(5)	0.9526(4)	4.5(6)
C20	0.2801(5)	0.3615(5)	0.5271(5)	4.6(6)	C61	0.0752(5)	0.2020(5)	0.8945(4)	2.8(5)
C21	0.3886(5)	0.2315(5)	0.5129(4)	2.9(5)	C62	0.1454(6)	0.2063(5)	0.8842(4)	4.0(6)
C22	0.3950(5)	0.1449(5)	0.4171(4)	3.0(5)	C63	0.1619(6)	0.1597(6)	0.8459(5)	5.0(7)
C23	0.4236(6)	0.0858(5)	0.4538(4)	4.1(6)	C64	0.1080(7)	0.1082(6)	0.8174(5)	5.6(7)
C24	0.4089(7)	0.0167(5)	0.4329(5)	5.2(7)	C65	0.0380(6)	0.1030(6)	0.8269(5)	4.9(6)
C25	0.3673(7)	0.0047(6)	0.3746(5)	5.9(8)	C66	0.0225(5)	0.1503(5)	0.8658(4)	3.4(5)

Crystal Data for 4·CH₂Cl₂: C₃₄H₃₂AuCl₃FeO₂P₂, MW = 893.74, monoclinic, space group *P*₂₁/*n*; *a* = 10.896(2), *b* = 21.064(6), *c* = 15.212(3) Å; β = 101.86(2)°, *V* = 3417(1) Å³; *Z* = 4, *F*(000) = 1572, *D*_{calcd} = 1.738 g/cm³; Nonius CAD-4 data, Mo radiation, λ = 0.710 69 Å, μ = 5.06 mm⁻¹; minimum and maximum transmission factors 0.479–0.999. The structure was solved by heavy atom methods and refined by full-matrix least squares (all non-hydrogen atoms anisotropic and hydrogen atoms idealized with C–H = 1.00 Å). *R* = 0.031, *R*_w = 0.039, and GOF = 1.86 with 75 atoms and 389 parameters for 3578 out of 4454 measured reflections, cut off *I*_o > 2.5σ(*I*_o).

Crystal Data for 5: C₃₄H₃₃AuFeO₂P₂, MW = 788.39, monoclinic, space group *P*₂₁/*n*; *a* = 16.606(2), *b* = 18.086(3), *c* = 21.629(5) Å; β = 100.62(1)°, *V* = 6384.8(20) Å³; *Z* = 8, *F*(000) = 3103, *D*_{calcd} = 1.640 g/cm³; Nonius CAD-4 data, Mo radiation, λ = 0.710 69 Å, μ = 5.16 mm⁻¹; minimum and maximum transmission factors 0.499–1.000. The structure was solved by heavy atom methods and refined by full-matrix least squares (all non-hydrogen atoms anisotropic and hydrogen atoms idealized with C–H = 1.00 Å). *R* = 0.034, *R*_w = 0.036, and GOF = 1.17 with 146 atoms and 722 parameters for 4809 out of 8324 measured reflections, cut off *I*_o > 2.5σ(*I*_o).

Crystal Data for 9·2CH₂Cl₂: C₃₅H₃₃Cl₆FeO₂P₂Rh, MW = 919.05, monoclinic, space group *P*₂₁/*a*; *a* = 18.406(3), *b* = 18.606(2), *c* = 23.915(4) Å; β = 109.28(2)°, *V* = 7731(2) Å³; *Z* = 8, *F*(000) = 3695.67, *D*_{calcd} = 1.579 g/cm³; Nonius CAD-4 data, Mo radiation, λ = 0.710 69 Å, μ = 1.33 mm⁻¹; minimum and maximum transmission factors 0.777–1.000. The structure was solved by direct methods and refined by full-matrix least squares (all non-hydrogen atoms anisotropic and hydrogen atoms idealized with C–H = 1.00 Å). *R* = 0.041, *R*_w = 0.041, and GOF = 1.53 with 176 atoms and 819 parameters for 5508 out of 10 086 unique reflections, cut off *I*_o > 2.5σ(*I*_o).

Acknowledgment. The authors take this chance to thank Academia Sinica and the National Science Council, ROC, for the kind financial supports.

Supporting Information Available: For the structures of 4, 5, and 9, listings of crystallographic data and refinement details, positional and anisotropic thermal parameters, and bond distances, angles, and structural parameters (43 pages). Ordering information is given on any current masthead page.

OM9409736